ADVANCED MATERIALS INTERFACES
Open Access
www.advmatinterfaces.de

Catalytic Activity of Horseradish Peroxidase Immobilized on Pristine and Two-Photon Oxidized Graphene

*Johanna Schirmer, Ester Iatta, Aleksei V. Emelianov, Maija Nissinen, and Mika Pettersson**

Biosensors based on graphene and bio-graphene interfaces have gained momentum in recent years due to graphene's outstanding electronic and mechanical properties. By introducing the patterning of a single-layer graphene surface by two-photon oxidation (2PO), the surface hydrophobicity/hydrophilicity and doping can be varied at the nanoscale while preserving the carbon network, thus opening possibilities to design new devices. In this study, the effect of 2PO on the catalytic activity of the noncovalently immobilized enzyme horseradish peroxidase (HRP) on single-layer graphene-coated Si/SiO_2 chips is presented. To monitor the activity continuously, a simple well-plate setup is introduced. Upon controllable 1–2-layer immobilization, the catalytic activity decreases to a maximum value of 7.5% of the free enzyme. Interestingly, the activity decreases with increasing 2PO area on the samples. Hence, the HRP catalytic activity on the graphene surface is locally controlled. This approach can enable the development of graphene-bio interfaces with locally varying enzyme activity.

1. Introduction

The immobilization of biomolecules has a wide range of applications, including biosensing, drug delivery, and industrial processes used in the production of pharmaceutical, chemical, and food products.[1,2] Additionally, immobilized biomolecules can improve a surface's biocompatibility for medical applications.[3] When proteins and enzymes are immobilized on a solid support, it is crucial to preserve their functionality and, for enzymes, their catalytic activity. Therefore, investigating the interactions between the protein or enzyme and the solid support and their effects on the functionality and catalytic activity is central in the research developing biocompatible surfaces and enzyme-based biosensors.

Support materials for enzymes include polymers and 2D materials, such as graphene and its derivatives.[2,4–6] Enzymes can be immobilized on the graphene materials covalently or noncovalently, with the latter being preferred as it preserves graphene's outstanding electronic and mechanical properties.[7] The noncovalent immobilization of enzymes on graphene oxide (GO) is based on dipole–dipole and ionic interactions between the enzyme and the oxygen-containing functional groups of GO as well as π–π stacking. For pristine graphene, noncovalent approaches commonly include linker molecules such as pyrene derivatives,[8–10] which are covalently attached to the enzyme and interact with graphene via π–π stacking. However, a direct attachment was also demonstrated for a dihydrolipoyl acyltransferase supramolecular complex and horseradish peroxidase (HRP).[11,12]

HRP is a 44 kDa, well-studied biosensing enzyme that has shown catalytic activity both free in solution and when immobilized on different support materials, including a pristine graphene surface[10] and GO flakes. [13] It catalyzes the oxidization reaction of its substrates by consuming hydrogen peroxide (H_2O_2). The catalytic activity of HRP was preserved after noncovalent immobilization on graphene and GO, although it was lower for the immobilized than for the free enzyme in the solution.[10,13] This was attributed to structural changes of HRP upon the noncovalent immobilization. However, the thermal and storage stability improved after the immobilization of HRP on GO.[14] On pristine graphene, the stability of HRP was lower compared to the free enzyme in the solution,[10] suggesting that the two graphene derivatives might interact differently with HRP.

Two-photon oxidation 2PO)[15] of graphene is a tool that allows for the combination of the properties of oxidized and pristine graphene on one surface with a nanoscale resolution. While the carbon network remains intact, mainly hydroxyl and epoxide groups are introduced on the graphene surface.[16] This method enables the design of new sensors and bio interfaces with graphene. So far, the tuning of the graphene field effect transistor sensitivity for pH sensing[17] and the tuning of protein immobilization[12] have been demonstrated. In detail, HRP adsorption on the surface happened preferably in the 2PO compared to the pristine areas and the immobilization affected

J. Schirmer, E. Iatta, A. V. Emelianov, M. Nissinen, M. Pettersson
Department of Chemistry
Nanoscience Center
University of Jyväskylä
Survontie 9 B, Jyvaskyla FI-40015, Finland
E-mail: mika.j.pettersson@jyu.fi

The ORCID identification number(s) for the author(s) of this article can be found under https://doi.org/10.1002/admi.202300870

DOI: 10.1002/admi.202300870

the doping level of graphene, demonstrating an electronic interaction. However, the question of whether the immobilized enzyme retains its catalytic activity remained open.

In this study, we combine the existing knowledge about HRP with 2PO of graphene to assess the catalytic activity of the enzyme. We noncovalently immobilized HRP on pristine and 2PO single-layer graphene surfaces and performed a kinetic analysis of an HRP-catalyzed reaction using ultraviolet-visible (UV–vis) spectroscopy. The results were correlated with the surface type. In this way, we demonstrate how 2PO of graphene can control the catalytic activity of HRP.

2. Experimental Section

2.1. Materials

HRP (Type VI, lyophilized, ≥250 units per mg), $Na_2HPO_4{\cdot}2H_2O$, and $NaH_2PO_4{\cdot}2H_2O$ were purchased from Merck. 3,3′,5,5′-tetramethylbenzidine (TMB) solution containing <0.1% H_2O_2 was purchased from Immunochemistry Technologies. All chemicals were used as described by the manufacturer and without further purification.

2.2. Graphene Samples

2.2.1. Single-Layer Graphene Surface Preparation

Graphene was synthesized on Cu (111) thin films evaporated onto single-crystal sapphire (0001) substrates. The catalyst film was annealed at 1060 °C under the gas flows of argon (470 sccm) and hydrogen (27 sccm) for 30 min to promote monocrystallinity through secondary grain growth. After annealing, graphene growth was initiated by adding 6.8 sccm of 1% methane in argon to the furnace while keeping the temperature at 1060 °C. The growth time was 25 min. The graphene films were transferred by a standard poly methyl methacrylate (PMMA) transfer method[18] onto a silicon substrate (2 mm x 2 mm) with a 300 nm thermal oxide film. The PMMA film was removed with acetone (30 min at 50 °C). Finally, the samples were annealed at 300 °C in Ar/H_2 atmosphere for 2 h to remove PMMA residues.

2.2.2. Two-Photon Oxidation

2PO of graphene was performed with a 515 nm femtosecond laser (Pharos-10, Light Conversion Ltd., 600 kHz repetition rate, 250 fs pulse duration, 6 nJ pulse energy, Lithuania) in an ambient atmosphere with a relative humidity of 45%. A high-speed galvanometer scanner (Newson, Belgium) with high numerical aperture optics with a focal length of 65 mm (Sill Optics, Germany) was utilized. To pattern the graphene areas, the scanner speed of 4 mm s^{-1} with a beam spot of 5 and 0.1 µm separation between lines was used. The laser parameters for the 2PO of graphene used in this work were optimized (to achieve the highest ID/IG ratio) as reported previously.[19,20] The oxidation was verified by Raman spectroscopy (Figure S1, Supporting Information).

2.3. Sample Characterization

2.3.1. Atomic Force Microscopy

Atomic force microscopy (AFM) imaging was performed in air on a Bruker Dimension Icon AFM, operated in PeakForce Tapping mode. Scan-Asyst-AIR probes (Bruker, USA) made from silicon nitride with a spring constant of 0.4 N m^{-1} were used, and the PeakForce Setpoint was 2 nN for all images. The images were processed and analyzed with the Nanoscope Analysis 1.9 software.

2.3.2. Raman Spectroscopy

The Raman spectra of pristine and laser-oxidized graphene were recorded with a DXR Raman (Thermo Scientific), equipped with a 50x objective. The excitation wavelength was 532 nm, and the laser power was 1 mW.

2.4. HRP Immobilization

Phosphate buffer saline (PBS, 0.2 M) was prepared by mixing a 0.2 M solution of $Na_2HPO_4 \cdot 2\ H_2O$ in deionized water with a 0.2 M solution of $NaH_2PO_4 \cdot 2\ H_2O$ until the desired pH of 7.1 was reached. HRP (1 mg, 250 units) was dissolved in 1 mL of PBS to obtain the enzyme stock solution (250 U mL^{-1}), which was diluted with PBS to obtain an HRP concentration of 1.25 U mL^{-1}.

The graphene samples were incubated in freshly prepared and diluted HRP solutions (2 mL) for 1 h at room temperature (rt), protected from light, before washing with PBS (3 × 1 mL).

Subsequently, each sample was mounted at the side wall of a well in a 96-well plate (polystyrene, Sarstaedt) using commercially available double-sided adhesive tape. PBS (300 µL) was added to each well for sample storage before the activity measurements to prevent the drying of the enzyme.

2.5. Catalytic Activity Measurements

All measurements were performed on a Spark multimode microplate reader (Tecan) in absorbance scan mode. The absorption spectra were measured between 200 and 800 nm wavelength, in the UV–vis spectral range, with a resolution of 2 nm. All spectra were baseline corrected. To exclude the interference of the tape and the sample, negative control experiments were performed (Figure S2, Table S1, Supporting Information).

2.5.1. Kinetic cycles

After immobilization of the enzyme, PBS (5 µL) was replaced by TMB solution (containing <0.1% H_2O_2) in the well containing the sample. Then, a kinetic loop absorbance scan was started, taking an absorption spectrum every 30 s for 30 min.

2.5.2. Stability over time

To assess the reusability of the immobilized HRP, the samples were stored overnight after the first kinetic cycle measurement.

The next day, 5 µL of solution was replaced by TMB solution (5 µL, containing <0.1% H_2O_2) in each well. A kinetic loop was measured as described above (Section 2.5.1.). The procedure was repeated on the following 2 days (4 days in total) until no catalytic activity was detected. After the last measurement, the liquid was removed from each well, and the samples were dried overnight at rt.

2.5.3. Calibration Curve

An HRP solution (2.5×10^{-5} µg µl^{-1}) was prepared from the HRP stock solution. For the calibration curve, nine wells in a 96-well plate were prepared as described in Table S2 (Supporting Information). TMB solution (5 µl, containing <0.1% H_2O_2) was added immediately before measuring absorption spectra every 30 s for 10 min.

2.5.4. Rate Calculation

From each spectrum, the maximum of the 655 nm absorption band was extracted and plotted against time after TMB addition. A linear fit was applied to the data points at the beginning of each measurement (usually the first 0.5–5 min). The slope of the fit (unit Abs min^{-1}) was defined as the reaction rate, with its standard deviation as the error of the rate. The Beer-Lambert law (1) and the volume of solution were used to convert the unit of the rate and its error to mmol min^{-1}:

$$c = \frac{A}{\epsilon \cdot l} \tag{1}$$

where A = the measured absorbance, ϵ = the extinction coefficient for the charge transfer complex (CTC; ϵ_{CTC} = 3.9×10^4 L mol^{-1} cm^{-1} (for the absorption at 655 nm)[21]), and l = the path length in the plate reader (0.9 cm).

2.6. HRP Coverage

To estimate the mass of HRP immobilized on the graphene samples, each dried sample was gently scratched with a spatula to remove both HRP and graphene from the Si/SiO_2 substrate. AFM images were recorded covering the protein layer and a part of a scratch (Figure S3, Supporting Information). From each sample, two or three images were recorded and compared with the AFM images before the HRP immobilization at the edge of the graphene sheet. The height differences between SiO_2 and graphene (h_{gr}) or HRP (h_{gr+HRP}), respectively, were measured with the Nanoscope Analysis 1.9 software step tool and used to calculate the height of the HRP layer h_{HRP}:

$$h_{HRP} = h_{gr+HRP} - h_{gr} \tag{2}$$

The obtained heights of the protein layer were compared to the dimensions of HRP (4.0 nm x 4.4 nm x 6.8 nm),[22] and the number of layers on each sample was determined.

To assess the relative area covered by the enzymes (*PC*), the bearing analysis tool of Nanoscope analysis was used. The tool gives the amount of data points above a certain, user-defined level in % (Figure S4, Supporting Information). The bearing level was set to h_{gr} to include only points above the graphene surface.

Assuming that HRP lays mainly on one of the longer sides, it would cover either 6.8 nm x 4.0 nm = 27.2 nm^2 or 6.8 nm x 4.4 nm = 29.92 nm^2. For further calculations, the mean of these two areas, 28.56 nm^2, was used as the area covered by one HRP enzyme (A_{HRP}). The mass of HRP m_{HRP} on each sample was estimated as follows:

$$m_{HRP} = \frac{\frac{A_{gr} \cdot PC}{A_{HRP}} \cdot M_{HRP}}{N_A} \tag{3}$$

where A_{gr} = the total area on a sample covered by graphene, M_{HRP} = the molar mass of HRP (44 kDa) and N_A = the Avogadro constant (6.022×10^{23} mol^{-1}).

2.7. Ethics Approval

The research and manuscript meet the ethical guidelines outlined in this journal's Author Guidelines, including adherence to the legal requirements of the study country

3. Results and Discussion

3.1. Setup

Measuring the catalytic activity of surface-immobilized enzymes with UV–vis spectroscopy has some practical challenges. The enzymes cannot be immobilized in the same container used to record the spectra, such as a cuvette or a well plate, since the enzymes would immobilize not only on the desired surface but also in the container itself. In an earlier approach, separate containers were used for catalytic reaction and absorption measurement.[10] However, this experiment design limits the number of possible measurements because the solution needs to be transferred for the measurement. The reaction cannot be monitored continuously, and consequently, reaction rates cannot be calculated. To monitor the reaction continuously, the sample must be mounted in the measurement container without disturbing the measurement. Here, we introduce a simple approach: We used double-sided adhesive tape to mount our 2 mm x 2 mm Si/SiO_2 chips coated with single-layer graphene and HRP into a 96-well plate and were able to continuously measure the progress of the HRP-catalyzed oxidation of TMB (**Figure 1**). The possible interference of the tape and the sample were excluded with negative control experiments (Figure S2, Table S1, Supporting Information).

3.2. HRP Loading

The noncovalent immobilization of proteins is based on physical interactions between the surface and the protein. Thus, controlling the amount of immobilized protein and its orientation is challenging. However, to sufficiently evaluate the catalytic activity of immobilized enzymes, it is crucial to know the enzyme load.

In our experiments, HRP was immobilized on three different graphene surfaces, which differ in the area of 2PO graphene:

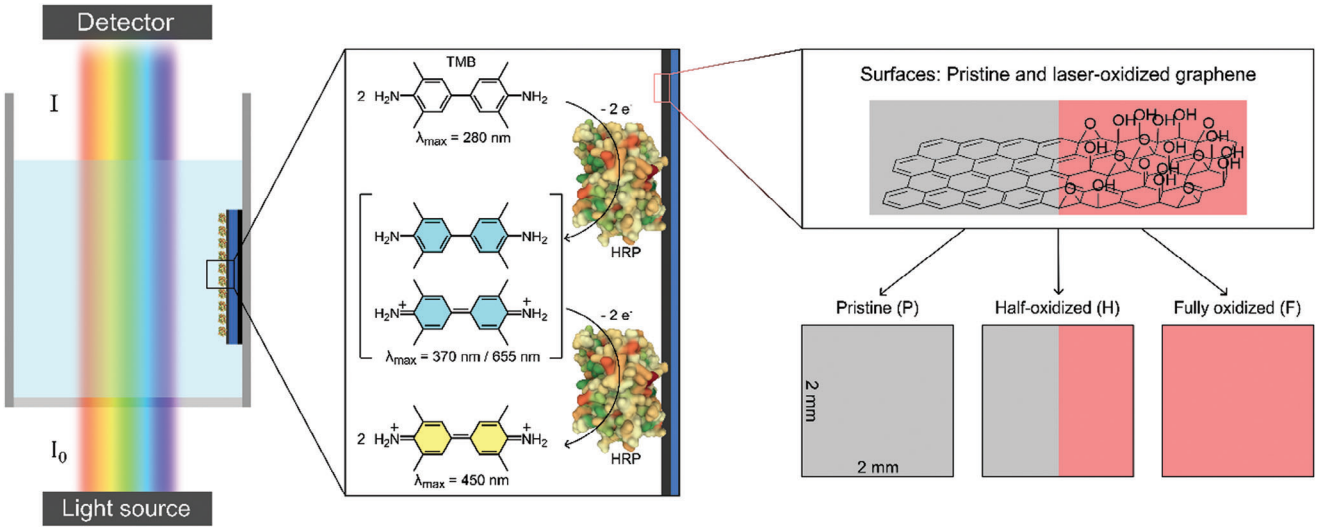

Figure 1. Schematic representation of the experiment: UV–vis absorption spectra were recorded from a well plate with a sample mounted on the side of the well. The sample consists of a graphene surface with noncovalently immobilized HRP enzyme, which oxidizes TMB if it is catalytically active. The two-step reaction can be observed in the UV–vis absorption spectra. Three distinct graphene surfaces were studied to see the effect of laser-oxidation on the catalytic activity of HRP.

pristine (P), half-oxidized (H), and fully oxidized (F) graphene (Figure 1). Our previous study showed that under certain conditions, HRP prefers to adsorb to the 2PO areas.[12]

Here, the amount of HRP on each sample was estimated as described in Section 2.6., using AFM images before and after the protein immobilization and extrapolating the whole area covered by graphene. (**Figure 2**, **Table 1**; Figure S3, Supporting Information). The amount of HRP varies between a monolayer and 2.5 layers, demonstrating that we were able to immobilize HRP noncovalently on graphene in a controlled manner in a range of a few layers on the pristine and 2PO graphene surfaces. In contrast to our previous study,[12] there was no clear preference toward one surface. This might be caused by different oxidation and immobilization conditions. Since the HRP layer does not cover the whole graphene surface for some samples, we calculated the protein coverage from the same AFM images (Table 1; Figure S4, Supporting Information), showing that HRP covered 84–100% of the graphene area. The graphene and 2PO areas were measured from optical microscope images and varied between the samples in the range from 2.76 to 3.62 mm^2 (total graphene area) and from 1.63 to 3.23 mm^2 (2PO area). The variation of the total graphene area originates from the graphene layer position on the surface after the transfer process. Considering the molar mass of HRP, m_{HRP} was calculated for each sample (Section 2.6., Table 1) and was found to vary from 4.41 to 19.94 ng. Thus, distinct catalytic activity differences could be expected from the samples due to a varying m_{HRP}.

3.3. Surface Effect on the Catalytic Activity of HRP

The catalytic activity and stability of HRP can be measured by following the oxidation of a substrate over time. TMB absorbs light in the UV–vis spectral region, with distinct absorbance maxima for each oxidation step (Figure 1). If HRP is active, TMB is oxidized under consumption of H_2O_2 from a diamine (TMB^0) to a diimine (TMB^{+2}) via the formation of a charge transfer complex (CTC). The monitoring of the arising absorption bands over

Table 1. Estimation of the total HRP mass (m_{HRP}) on each sample and values used for the calculation, with the height of the HRP layer h_{HRP}.

	h_{HRP} [nm]	#HRP layer	Protein Covering [%]	Graphene area [mm^2]	2PO area [mm^2]	m_{HRP} [ng]
P1	3.5	1	89	2.76	0	4.41
P2	3.5–6.6	1.5	100	3.62	0	13.89
P3	8.4–10.6	2.5	100	3.12	0	19.94
H1	5.1–6.4 (2PO), 3.9 (pristine)	1.5 (2PO) 1 (pristine)	98 (2PO) 99 (pri)	3.36	1.68	10.54
H2	5.0–5.4 (2PO), 3.9 (pristine)	1.5 (2PO) 1 (pristine)	98 (2PO) 95 (pristine)	3.13	1.78	9.99
H3	5.9–7.3 (2PO), 4.2–6.4 (pristine)	1.5 (2PO) 1.5 (pristine)	84 (2PO) 100 (pristine)	2.94	1.63	10.32
F1	8.5	2	99	3.23	3.23	16.33
F2	4.4–5.7	1	97	2.93	2.93	7.39

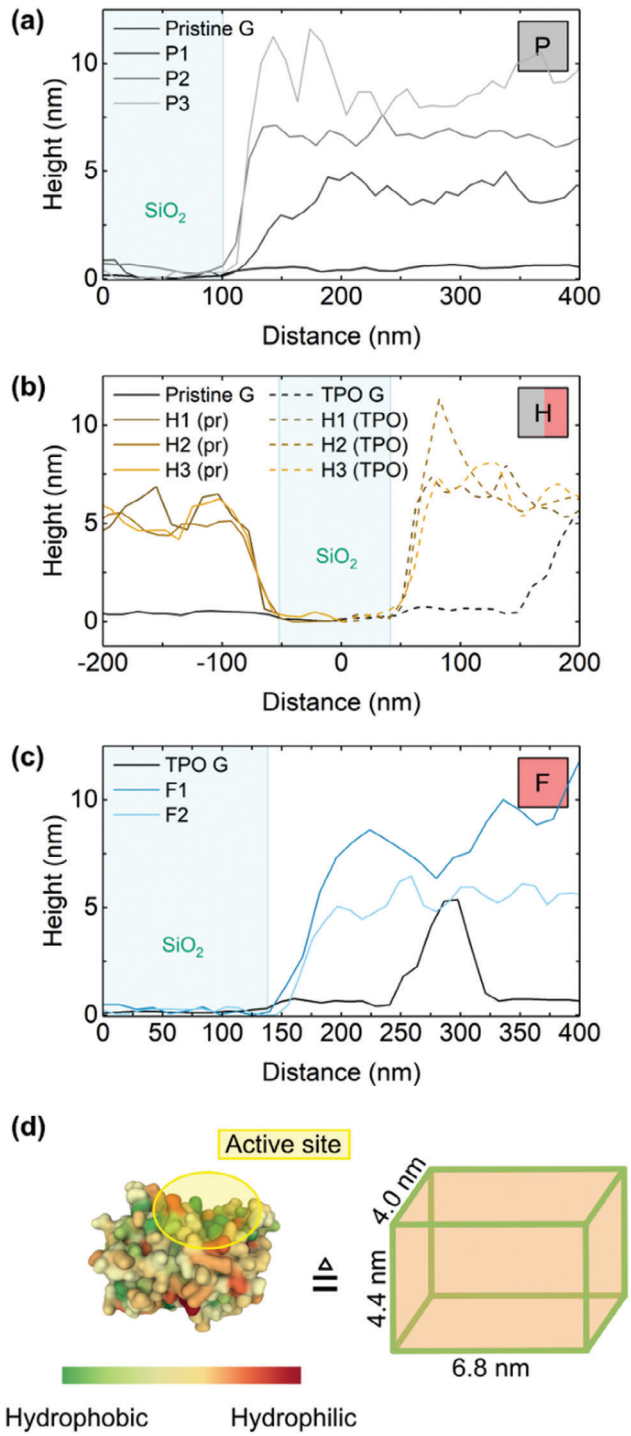

Figure 2. a–c) Example AFM topography cross sections from all samples and pristine and 2PO graphene (G) as a base for the estimation of the HRP mass on each sample. The corresponding AFM images are shown in Figure S3 (Supporting Information). d) Crystal structure of HRP in the Gaussian surface view, showing hydrophobic and hydrophilic amino acid residues,[23–25] and the simplified cuboid model used for HRP mass calculations.

time elucidates the reaction progress. On day 1, the absorption bands of the CTC (370 and 655 nm) were observed for all samples 10 min after the addition of TMB and H_2O_2 (**Figure 3**a–c), demonstrating catalytically active HRP on all three surface types. The formation of TMB^{+2} was observed on all samples except for F1 (450 nm absorption band). Indeed, as expected due to the varying mass of HRP on the samples, the band intensities clearly vary between the sample type and the single samples. To quantitatively compare the catalytic activity of HRP on the samples, the oxidation reaction rate from TMB^0 to CTC was calculated using the absorption maximum at 655 nm due to its minimal overlap with other bands (Figure 3d; Table S3, Supporting Information). A general trend shows decreasing rates with increasing oxidized area (P to F). To eliminate the varying enzyme load of the samples from the calculated values, the rates were divided by the calculated mass of HRP for each sample (Figure 3e, Table 1; Table S3, Supporting Information). The trend remains for the normalized rate values. These results show that 2PO of the graphene surface reduces the catalytic activity of noncovalently bound HRP.

When binding noncovalently to a surface, certain amino acid residues interact with certain surface features. Depending on the strength of interaction and stability of the protein, the tertiary structure of a protein may be altered, and—in the case of enzymes—the function may be lost. Indeed, according to previous experimental and theoretical results α-helical structural motifs tend to change their structure on pristine graphene in contrast to β-sheets, which are less affected.[26–28] HRP consists predominantly of α-helices and is prone to these effects. In 2PO graphene, the carbon network is largely preserved despite introducing oxygen-containing groups.[15,16] Hence, similar effects could trigger structural changes and loss of function in HRP on both pristine and 2PO graphene. However, lower reaction rates on samples with 2PO graphene indicate that the effects are more significant after 2PO of the surface, i.e., the structure of the enzyme is perturbed more on 2PO than on pristine graphene.

In addition, HRP could lose its activity due to the blocking of the active site by the support material or other enzymes.[28,29] In our noncovalent approach, the orientation of the enzymes approaching the surface is random, and a part of the immobilization might occur with the active site facing the surface. Blocking the active site by the graphene surface itself is, therefore, possible for both surfaces. Blocking HRP's active site by other enzymes is possible for samples with more than one protein layers. The upper layer could make the active sites of the lower layer inaccessible for the substrate.

To estimate the catalytic activity of the immobilized HRP on each sample, we compared the rates of the immobilized enzymes to the rate of free HRP. A calibration curve was generated by measuring the reaction rate from TMB^0 to CTC from nine solutions with distinct, known masses of HRP and fitting a linear curve to the rate values (**Figure 4**a). Knowing the reaction rate, the mass of active HRP on each sample was calculated with the linear fit equation (Figure 4b). The estimated masses of active HRP vary between 0.06 ng (F1) and 0.96 ng (P3).

To further classify the amount of active HRP on each sample, the mass of active HRP was related to the previously calculated total mass of HRP on each sample (**Table 2**). Overall, the activity of the immobilized HRP was a maximum of

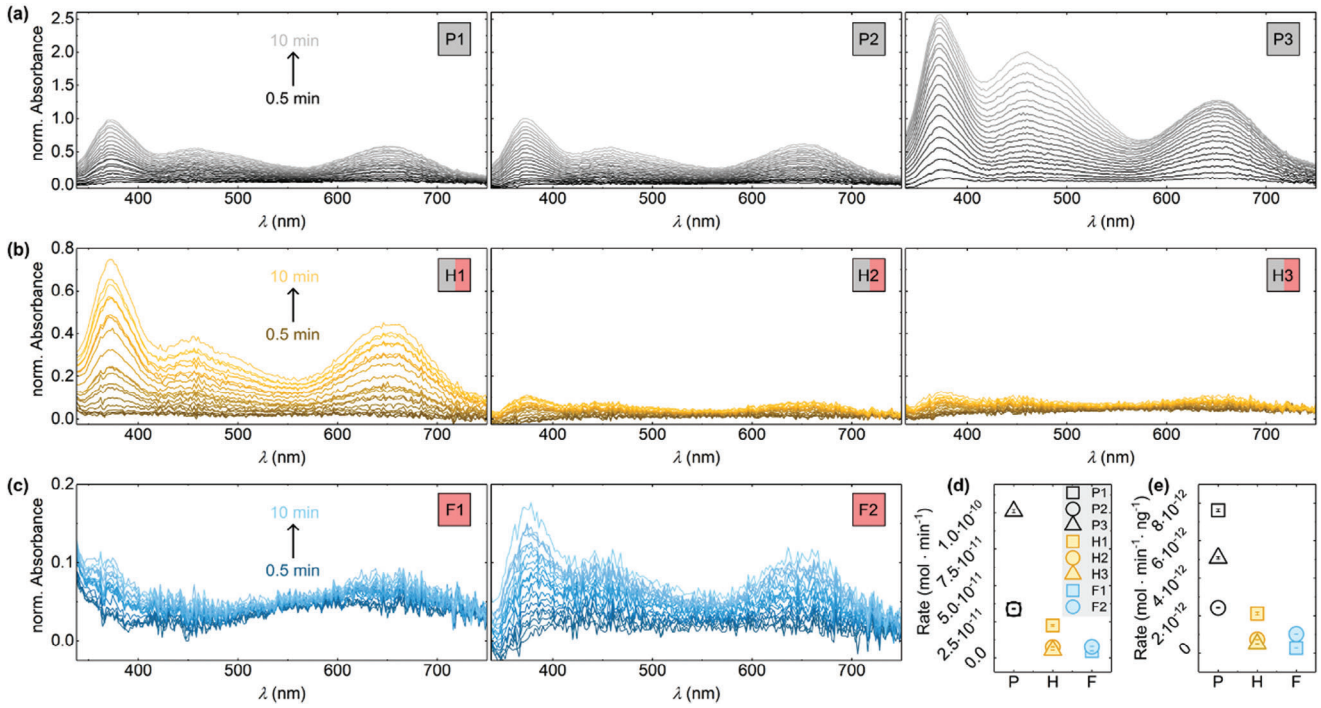

Figure 3. a–c) Normalized absorption spectra from the first 10 min after substrate addition on day 1 for each sample. Sample name and color gradient are indicated in the plots. d) Reaction rates for the oxidation of TMB^0 to CTC on day 1 for eachsample. e) Reaction rates of (d) normalized to m_{HRP} (Table 1). Error bars indicate the standard deviation of the calculated rates.

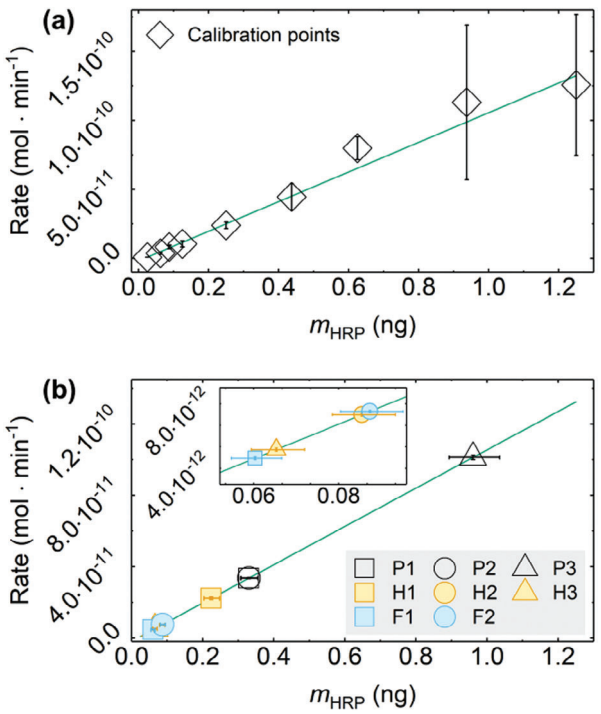

Figure 4. a) Calibration points (black squares) and resulting linear calibration fit (green). Error bars present the standard deviation of each rate. The linear fit equation was Rate = $m_{HRP} \cdot (1.1 \times 10^{-10} \pm 6.4 \times 10^{-12}) - (1.9 \times 10^{-12} \pm 1.6 \times 10^{-13})$ b) Calibration fit from (a) and calculated m_{HRP} for each sample. Error bars indicate the maximum and minimum mass of HRP.

7.5% of the free enzyme (P1). The activity loss might originate from the surface-induced structural changes or the blocking of the active site, as suggested above.[26–29] Looking at the samples in detail, the biggest mass-normalized activity was found on the pristine samples P1, P3, and P2, respectively. The mass-normalized activity of HRP on the half-oxidized samples is in a similar range as on the fully oxidized samples. Considering that perhaps only the top layer of HRP is accessible for the substrate, the mass-normalized activity of HRP would change to 7.5% (P1), 3.6% (P2) and 12.0% (P3) for pristine samples, 2.6% (H1), 1.2% (H2) and 1.0% (H3) for half-oxidized samples and 0.73% (F1) and 1.2% (F2) for fully oxidized samples. These values are in a similar range than before and follow the same trend. The results indicate that, compared to pristine graphene, the interactions between 2PO graphene and HRP

Table 2. Mass-normalized activity of HRP as a ratio of the mass of active HRP $m_{HRP,active}$ and the total mass of HRP m_{HRP} for each sample.

	m_{HRP} [ng]	$m_{HRP,active}$ [ng]	Mass-normalized activity [%]
P1	4.41	0.33	7.5
P2	13.89	0.33	2.4
P3	19.94	0.96	4.8
H1	10.54	0.22	2.1
H2	9.99	0.09	0.90
H3	10.32	0.07	0.68
F1	16.33	0.06	0.37
F2	7.39	0.09	1.2

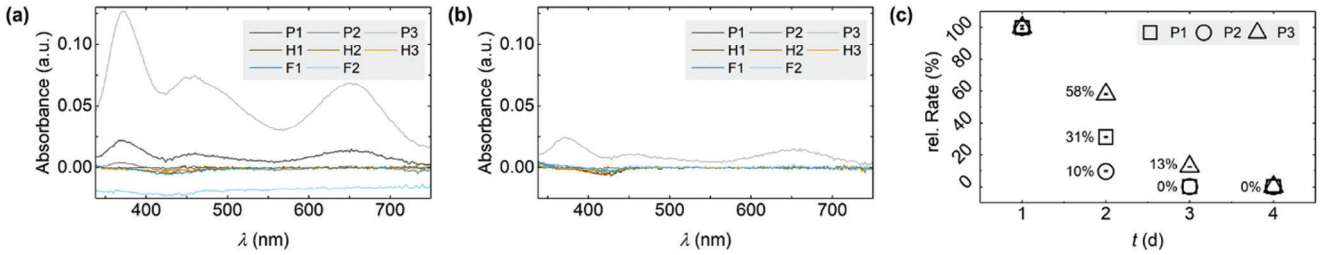

Figure 5. Catalytic activity of HRP over time: Absorption spectra 10 min after substrate addition of all samples on a) day 2 and b) day 3. c) Reaction rates relative to day 1 for the oxidation of TMB^0 to CTC from day 1 to 4 for the three pristine samples. Error bars indicate the standard deviation of each rate. The exact values are shown in Table S4 (Supporting Information).

lead to either more HRP binding to the surface with the active site inaccessible for the substrate or a more significant impact on the enzyme structure and a consequent loss of function. Whether we analyze the raw data or include the graphene area, the HRP mass or the monolayer theory into our calculations, the results are the same: HRP was less active on 2PO graphene compared to the pristine graphene. However, the activity was not lost completely, and HRP on 2PO graphene can perform its enzymatic function. Thus, with 2PO of graphene, we can control the catalytic activity of the model enzyme HRP, which suggests that there might be similar effects on other proteins as well.

3.4. Stability of the Samples

To assess the stability of the noncovalently immobilized HRP on pristine and 2PO graphene, the catalytic activity measurement was repeated on the three following days after the incubation. The samples were stored in the solution overnight to prevent drying of HRP. The absorption spectra 10 min after the substrate addition show activity only for the three P samples on day 2 (**Figure 5**a) and on day 3 only for sample P3 (Figure 5b). On day 4, no catalytic activity was detected for any sample (Figure S5, Supporting Information). The corresponding reaction rates of the P samples present a decreasing activity over time for each sample (Figure 5c; Table S4, Supporting Information). On day 2, the activity had decreased relative to day one to 10% (P2), 31% (P1) and 58% (P3). P3 shows 13% of its initial activity on day 3. The decrease for the oxidized samples is 100% from day 1 to day 2, which could be caused by the already small initial activity, i.e., a possible activity on day 2 would be below the detection limit of the experiment. For our samples, the desorption of HRP from the surfaces can be neglected due to extensive washing after HRP immobilization. We, therefore, attribute the catalytic activity loss over time to structural changes of the immobilized enzymes. Blocking of the active site, as described above, might not happen after the initial immobilization of the enzymes, as noncovalent interactions should hold them in place. For the free enzyme, Hou et al. reported a remaining activity of roughly 40% after 12 h at 20 °C,[10] which is in the same range as our pristine samples after 24 h at rt. Therefore, the stability of HRP on pristine graphene is similar or better compared to the free enzyme. Hence, our results support the hypothesis of structural changes due to interactions between surface and HRP and are consistent with previous experimental and theoretical results for HRP on pristine graphene and graphene oxide flakes.[10,14,26]

4. Conclusion

In this study, we controllably immobilized HRP on single-layer graphene surfaces on Si/SiO_2 chips and demonstrated the effect of 2PO of the graphene surface on the catalytic activity of HRP. With our noncovalent approach, we were able to controllably immobilize 1–2 layers of HRP on both pristine and 2PO graphene in the nanogram scale. The catalytic activity was measured for the HRP catalyzed oxidation of TMB and observed via UV–vis spectroscopy. To continuously monitor the oxidation, we introduced a simple setup where the graphene sample was mounted to the wall of the measurement container. In this way, we could calculate reaction rates that correlate with the catalytic activity of the samples. The initial activity of the immobilized enzyme showed a clear trend of decreasing activity with increasing 2PO area. We attribute this to distinct interactions between HRP and the two surfaces, which differ in functional groups and the extent of *p*-type doping. Over the following three days, the activity steadily decreased for all pristine samples, while the oxidized samples lost their activity entirely after day 1. These results are consistent with the previous studies, which connect the activity loss to structural changes in the enzyme upon immobilization.

We demonstrated that 2PO of graphene affects the activity of HRP. In a previous study, we showed that the adhesion of HRP and bovine serum albumin on graphene surfaces can be tuned with 2PO.[12] Though these studies demonstrate the effects for one or two proteins, respectively, we believe that similar effects could be found for other proteins as they consist of similar amino acids that can interact with the surface. Herein, distinct secondary structure elements and 2PO levels might lead to different effects on the protein adhesion, function, and stability. Hence, 2PO as an optical, locally defined nanoscale method enables the construction of surfaces with differing protein loading and functionality. Our approach was performed for graphene, GO and HRP on a Si chip configuration and opens new possibilities for the design and development of biosensors and bio-graphene interfaces on Si chips.

Supporting Information

Supporting Information is available from the Wiley Online Library or from the author.

Acknowledgements

This work was funded by Jane and Aatos Erkko Foundation. The authors would like to thank Jane and Aatos Erkko Foundation for supporting the

work, Olli Rissanen for the production of the graphene samples, and Dr. Pasi Myllyperkiö for the design and development of the oxidation laser setup.

Conflict of Interest

The authors declare no conflict of interest.

Data Availability Statement

The data that support the findings of this study are available from the corresponding author upon reasonable request.

Keywords

catalytic activity, graphene, graphene-bio interfaces, protein immobilization, two-photon oxidation

Received: October 15, 2023
Published online:

[1] H. M. Fahmy, E. S. Abu Serea, R. E. Salah-Eldin, S. A. Al-Hafiry, M. K. Ali, A. E. Shalan, S. Lanceros-Méndez, *ACS Biomater. Sci. Eng.* **2022**, *8*, 964.
[2] A. Basso, S. Serban, *Mol. Catal.* **2019**, *479*, 110607.
[3] S. Bose, S. F. Robertson, A. Bandyopadhyay, *Acta Biomater.* **2018**, *66*, 6.
[4] N. Rohaizad, C. C. Mayorga-Martinez, M. Fojtu, N. M. Latiff, M. Pumera, *Chem. Soc. Rev.* **2021**, *50*, 619.
[5] H. Seelajaroen, A. Bakandritsos, M. Otyepka, R. Zboril, N. S. Sariciftci, *ACS Appl. Mater. Interfaces* **2020**, *12*, 250.
[6] Y. Wang, S. Di, J. Yu, L. Wang, Z. Li, *J. Mater. Chem. B* **2023**, *11*, 500.
[7] A. K. Geim, K. S. Novoselov, *Nat. Mater.* **2007**, *6*, 183.
[8] M. Singh, M. Holzinger, M. Tabrizian, S. Winters, N. C. Berner, S. Cosnier, G. S. Duesberg, *J. Am. Chem. Soc.* **2015**, *137*, 2800.
[9] K. Besteman, J.-O. Lee, F. G. M. Wiertz, H. A. Heering, C. Dekker, *Nano Lett.* **2003**, *3*, 727.
[10] B. Hou, A. D. Radadia, *ACS Biomater. Sci. Eng.* **2018**, *4*, 675.
[11] A. Alshammari, M. G. Posner, A. Upadhyay, F. Marken, S. Bagby, A. Ilie, *ACS Appl. Mater. Interfaces* **2016**, *8*, 21077.
[12] E. D. Sitsanidis, J. Schirmer, A. Lampinen, K. K. Mentel, V.-M. Hiltunen, V. Ruokolainen, A. Johansson, P. Myllyperkiö, M. Nissinen, M. Pettersson, *Nanoscale Adv.* **2021**, *3*, 2065.
[13] J. Zhang, F. Zhang, H. Yang, X. Huang, H. Liu, J. Zhang, S. Guo, *Langmuir* **2010**, *26*, 6083.
[14] F. Zhang, B. Zheng, J. Zhang, X. Huang, H. Liu, S. Guo, J. Zhang, *J. Phys. Chem. C* **2010**, *114*, 8469.
[15] J. Aumanen, A. Johansson, J. Koivistoinen, P. Myllyperkiö, M. Pettersson, *Nanoscale* **2015**, *7*, 2851.
[16] A. Johansson, H.-C. Tsai, J. Aumanen, J. Koivistoinen, P. Myllyperkiö, Y.-Z. Hung, M.-C. Chuang, C.-H. Chen, W. Y. Woon, M. Pettersson, *Carbon* **2017**, *115*, 77.
[17] A. Lampinen, E. See, A. Emelianov, P. Myllyperkiö, A. Johansson, M. Pettersson, *Phys. Chem. Chem. Phys.* **2023**, *25*, 10778.
[18] J. W. Suk, A. Kitt, C. W. Magnuson, Y. Hao, S. Ahmed, J. An, A. K. Swan, B. B. Goldberg, R. S. Ruoff, *ACS Nano* **2011**, *5*, 6916.
[19] A. V. Emelianov, D. Kireev, A. Offenhäusser, N. Otero, P. M. Romero, I. I. Bobrinetskiy, *ACS Photonics* **2018**, *5*, 3107.
[20] K. K. Mentel, A. V. Emelianov, A. Philip, A. Johansson, M. Karppinen, M. Pettersson, *Adv. Mater. Interfaces* **2022**, *9*, 2201110.
[21] P. D. Josephy, T. Eling, R. P. Mason, *J. Biol. Chem.* **1982**, *257*, 3669.
[22] D. Feng, T.-F. Liu, J. Su, M. Bosch, Z. Wei, W. Wan, D. Yuan, Y.-P. Chen, X. Wang, K. Wang, X. Lian, Z.-Y. Gu, J. Park, X. Zou, H.-C. Zhou, *Nat. Commun.* **2014**, *6*, 5979.
[23] G. I. Berglund, G. H. Carlsson, J. Hajdu, A. T. Smith, H. Szoke, A. Henriksen, *Nature* **2002**, *417*, 463.
[24] H. M. Berman, *Nucleic Acids Res.* **2000**, *28*, 235.
[25] D. Sehnal, S. Bittrich, M. Deshpande, R. Svobodová, K. Berka, V. Bazgier, S. Velankar, S. K. Burley, J. Koca, A. S. Rose, *Nucleic Acids Res.* **2021**, *49*, W431.
[26] J. Guo, X. Yao, L. Ning, Q. Wang, H. Liu, *RSC Adv.* **2014**, *4*, 9953.
[27] J. Katoch, S. N. Kim, Z. Kuang, B. L. Farmer, R. R. Naik, S. A. Tatulian, M. Ishigami, *Nano Lett.* **2012**, *12*, 2342.
[28] C. Garcia-Galan, Á. Berenguer-Murcia, R. Fernandez-Lafuente, R. C. Rodrigues, *Adv. Synth. Catal.* **2011**, *353*, 2885.
[29] L. Cao, *Carrier-bound Immobilized Enzymes*, Wiley-VCH, Weinheim, Germany **2005**.